Available online at www.sciencedirect.com

ScienceDirect

Ceramics International 40 (2014) 4529–4533

CERAMICS INTERNATIONAL

www.elsevier.com/locate/ceramint

The effect of argon shielding gas at plasma spray process on the structure and properties of $MoSi_2$ coating

Mohammad Erfanmanesh*, Saeed Reza Bakhshi, Mohammad Khajelakzay, Mostafa Salekbafghi

Department of Materials Science and Engineering, Malek Ashtar University of Technology, Shahin Shahr, Iran

Received 4 July 2013; received in revised form 28 August 2013; accepted 29 August 2013
Available online 7 September 2013

Abstract

In this work, $MoSi_2$ powder was agglomerated for using it in atmospheric plasma spray (APS) process. $MoSi_2$ coatings were manufactured by APS and argon-shrouded plasma spray (ASPS) processes. Phase composition and structural properties of coatings were analyzed using X-ray diffraction (XRD) and scanning electron microscopy (SEM). Also, the mechanical properties of coatings (such as microhardness and adhesion strength) were evaluated. Using the ASPS method, the coatings were found to have a low porosity and highly homogeneous structure. In addition, the argon protection gas was used to prevent the oxidation of the powder. Finally, the ASPS method revealed better microhardness and bending strength results for the corresponding tests.

Keywords: $MoSi_2$ coating; Atmospheric plasma spray; Agglomeration; Argon shielding gas

1. Introduction

$MoSi_2$ has been studied extensively as a potential high temperature structural material considering its favorable properties, including high melting point (2030 °C), low density (6.24 g cm^{-3}), extremely high resistance to oxidation and corrosion, and high electrical and thermal conductivity [1]. Moreover, it is well recognized that $MoSi_2$ is an attractive wear resistant material for application at room and high temperatures in corrosive and oxidative environments because of its high hardness and elastic modulus [2]. However, poor fracture toughness at ambient temperature (2–3 MPa $m^{1/2}$) and low strength at elevated temperature have seriously limited the development of the $MoSi_2$ matrix structural materials [3]. Many techniques have been suggested to deposit $MoSi_2$ coatings; e.g., chemical vapor deposition (CVD) [4], high velocity oxygen fuel (HVOF) [5], pulsed laser ablation and deposition (PLAD) [6], atmospheric (APS) and vacuum plasma spray (VPS) [7–9]. Among several coating manufacturing methods, plasma spraying is recognized as a highly efficient technology since it enables processing of a large number of coating materials, such as refractory materials. It can be an appropriate method for producing the protective coatings, because of its ability to coat large surfaces with a thick coating at high deposition rate and relatively low operating cost in comparison to the most of other coating deposition techniques [7]. The APS application is generally related to wear and corrosion protections, which are often based on oxide and carbide ceramic materials. Furthermore, APS technology also deals with processing of the metal and oxygen sensitive coating materials such as $MoSi_2$ [7].

Here, very little has been done upon application of atmospheric plasma spray process on $MoSi_2$ [7–9] and there exists no report in the case of ASPS for the protection from coating oxidation. In this study, the produced $MoSi_2$ powder was agglomerated and then the agglomerated $MoSi_2$ powder was sprayed by APS and argon-shrouded plasma spray (ASPS) processes. After that, phase and structural properties of the coatings were examined using X-ray diffraction (XRD) and a scanning electron microscope (SEM). Moreover, the mechanical properties of the coatings such as adhesion strength and microhardness were investigated.

2. Experimental methods

$MoSi_2$ powders were synthesized by milling and subsequent heat treatment [10]. The powder mixture of Mo and Si was prepared at the stoichiometric composition of nanocrystalline

*Corresponding author. Tel.: +98 3125912307; fax: +98 3125228530.
E-mail addresses: erfanmanesh@mut-es.ac.ir, erfanmanesh_m64@yahoo.com (M. Erfanmanesh).

0272-8842/$ - see front matter © 2013 Elsevier Ltd and Techna Group S.r.l. All rights reserved.
http://dx.doi.org/10.1016/j.ceramint.2013.08.128

$MoSi_2$ (the molar ratio of Mo:Si is equal to 1:2), and the powder was milled for 20 h under Ar atmosphere in an attritor mill with a rotational speed of 365 rpm. Mechanically alloyed (MAed) powders were heated in an Ar atmosphere controlled furnace at 1100 °C, for 7 h with a heating rate of 10 C/min.

Because the synthesized powders did not have a suitable flow for plasma spraying, they were agglomerated by Carboxy Methyl Cellulose (CMC) binder and the powders were sifted to the grain size fraction from 75 μm to150 μm. The coating deposition was carried out by the atmospheric spray system (Metallisation Plasma PS50M-PC, UK) equipped with a PS50MPF/B torch. To prevent oxidation of powders during spray, a spray torch with argon shielding gas (ASPS) was used. Then, the obtained results were compared with those of unprotected plasma spray. Table 1 summarizes the spray parameters which were optimized with respect to the adhesion strength. The carbon steel (Table 2), selected as substrate in this work, was grit-blasted by SiC particles of 20 meshes with 10 cm distance from the nozzle to sample for 20 s with 90° and then cleaned with ethanol prior to the spraying process. The average roughness (R_a) of the substrate was 9.72 ± 2 μm after grit blasting. Fig. 1 shows a schematic view of the ASPS method.

Microhardness measurements were made on polished cross-section of the samples. In this regard, a Zwick type (3212, Germany) device with a diamond of Vickers geometry was utilized. The load of 0.5 N was applied 15 s on the sample and the Vickers microhardness determined as HV0.05. The roughness of coatings was measured after spray operation using the fully automatic Mitutoyo machine. Adhesion strength of coatings was measured according to ASTM C0633 [11] using a universal Zwick puller device with the speed of 1 mm/min and adhesive resin from Scotch-Weld Company (SW2214 code). The cylindrical samples were used for plain carbon steel with a diameter of 2.5 cm, height of 3.5 cm, and coating thickness of 350 ± 25 μm. To determine microhardness, roughness, and adhesion strength of the samples, the tests were repeated on three samples and their average was presented. Crystalline phases of synthesized powders and coating were analyzed using XRD (PW-1877, Philips) operating with Cu Kα ($\lambda = 1.5405$ nm) radiation. The scan ranges from 20° to 90°, with a step size of 0.05°, and counting time of 1 s was applied at each step. The morphologies of coatings were evaluated by SEM (VEGA-XMU, Tescan). The porosity content of as-sprayed coatings was measured on polished cross-sections (resolution: 270 PPI) using the image analysis (ImageJ software). In this regard, five measurements were made for each sample. The actual relative volume fractions (RF) of phases can be calculated using the relative intensity (I) ratios of the strongest peaks obtained from XRD patterns for each phase, according to the following equation [12]:

$$\mathrm{RF\%\ phase} = I_{\mathrm{phase}} / (I_{MoSi_2(\alpha)} + I_{MoSi_2(\beta)} + I_{Mo_5Si_3} + I_{MoO_3(\alpha)} + I_{SiO_2}). \quad (1)$$

Table 1
Atmospheric plasma operating parameters of $MoSi_2$ coating.

Parameters	
Power (kW)	35
Gas Ar (slpm)	30
Gas N_2 (slpm)	5
Spray distance (cm)	10
Carrier gas Ar (slpm)	3
shroud gas flow (slpm)	5
Powder feed rate (g/min)	12
Substrate average temperature during deposition (°C)	< 150

3. Results and discussion

Fig. 2 shows XRD pattern of the powder and coatings applied on steel using the APS and ASPS techniques. A comparison

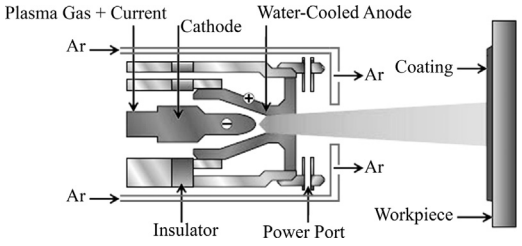

Fig. 1. A schematic drawing of the ASPS gun.

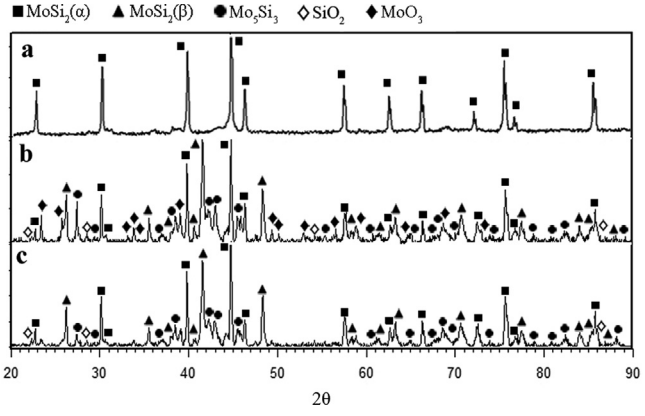

Fig. 2. X-ray diffraction diagrams of (a) powder $MoSi_2$, (b) plasma spray coating without protective gas and (c) plasma spray coating with using the ASPS method.

Table 2
The carbon steel chemical analysis.

Substrate	Chemical analysis (wt%)													
	Ti	Nb	Hf	Cr	Co	Al	S	P	Si	C	Mn	Mo	Ni	Fe
Carbon steel	–	–	–	–	–	–	0.015	0.018	0.182	0.136	0.625	0.025	0.047	98.925

between the results of XRD patterns of powder before and after the spray revealed that composition of powder significantly changes after spray. In addition to $MoSi_2$ (α), other phases such as $MoSi_2$ (β), Mo_5Si_3, MoO_3 and SiO_2 appeared in the XRD patterns after the spray. $MoSi_2$ (β), which is a metastable phase at room temperature, is considered as high temperature modification (β-modification) of molybdenum disilicide with a hexagonal lattice. Furthermore, existence of Mo_5Si_3, MoO_3 and SiO_2 phases might be attributed to the oxidation of $MoSi_2$ which takes places as follows:

$$5MoSi_2(s)+7O_2(g)\rightarrow Mo_5Si_3(s)+7SiO_2(s) \quad (2)$$

$$2MoSi_2(s)+7O_2(g)\rightarrow 2MoO_3(s)+4SiO_2(s) \quad (3)$$

Table 3
The relative fractions of each phase formed at unprotected and protected coatings.

Methods	Relative fraction (%)				
	$MoSi_2$ (α)	$MoSi_2$ (β)	Mo_5Si_3	SiO_2	MoO_3
ASPS	45	40	13.5	1.5	–
APS	37	37.5	16	3	6.5

The derived results are in good agreement with those of previous investigations [7,9]. XRD patterns of ASPS samples exhibited that the SiO_2, MoO_3, and Mo_5Si_3 peaks are smaller than those of the APS samples (Table 3), implying more $MoSi_2$ is oxidized during APS process. Fei et al. [7] reported that $MoSi_2$ coatings manufactured by an atmospheric plasma spray process are more oxidized as compared to the state of applying vacuum plasma spray process. However, it must be noted that the produced samples do not have a high degree of density.

Fig. 3 illustrates surface morphologies of as-sprayed $MoSi_2$ coatings using the APS and ASPS methods. Well-flattened lamellar morphologies were observed along with some spherical features on the surfaces of both coatings, indicating the typical morphologies of plasma sprayed coatings, except for splats formed through solidification of fully molten powders. Also, the partially molten powders were seen on the coating surface. However, APS coatings exhibit a higher number of microcracks compared to ASPS coatings (Fig. 3). These cracks can be attributed to the internal residual stresses generated during the spraying process [7], particle shrinkage due to a high cooling rate of the liquid–solid, and the coefficient of thermal expansion mismatch between the coating and the substrate [13]. The thermal expansion of the tetragonal Mo_5Si_3 is highly anisotropic, and is unfavorable since it produces microcracks [7].

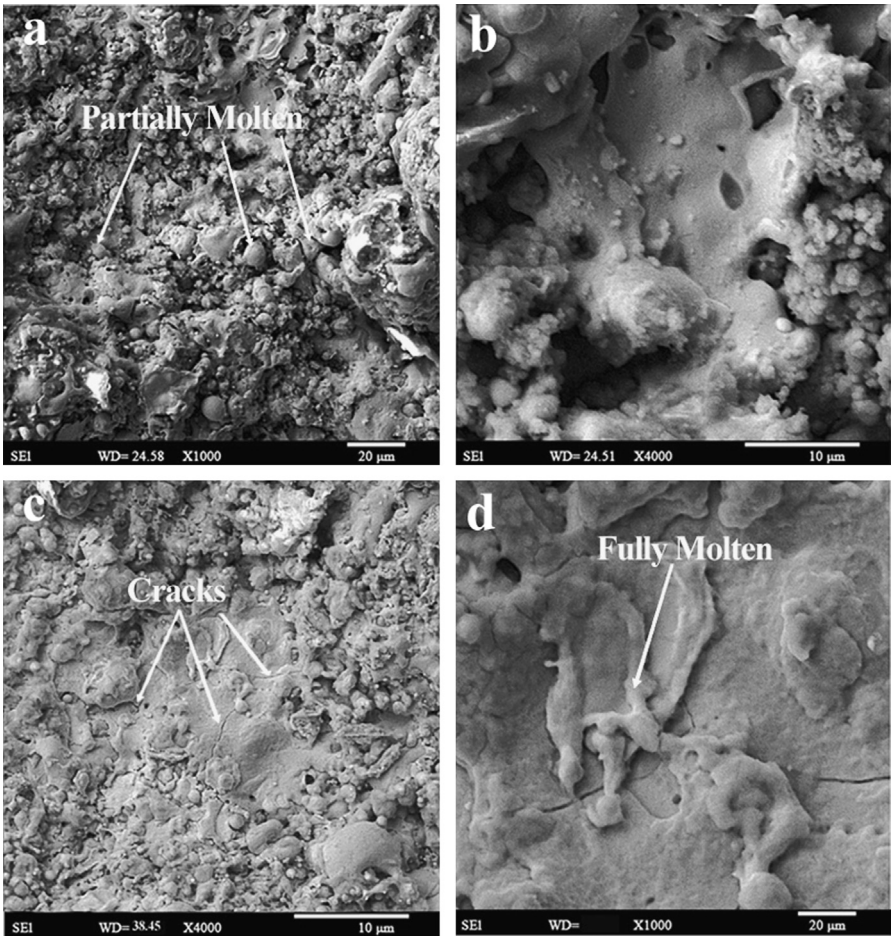

Fig. 3. Scanning electron microscope images of (a) & (b) surface morphology of ASPS and (c) & (d) APS method.

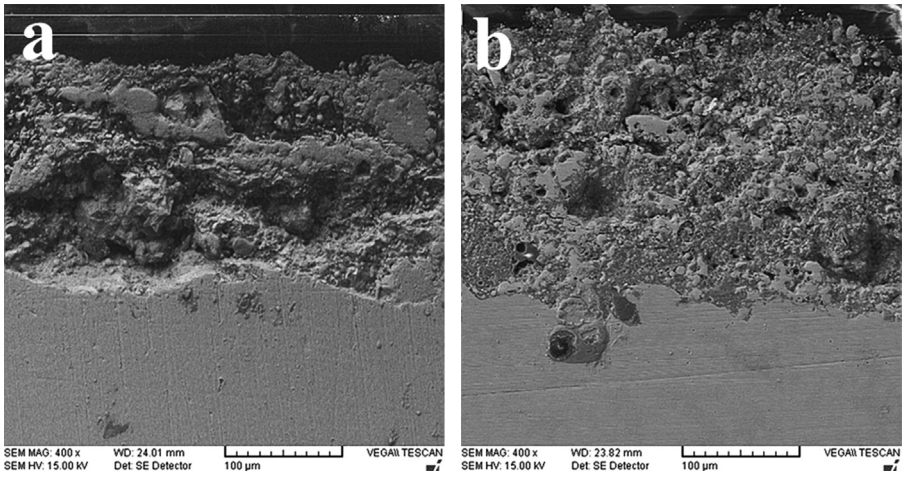

Fig. 4. Scanning electron microscope images of the cross section (a) unprotected and (b) protected coating.

Table 4
Results of roughness, microhardness and adhesion strength for protected and unprotected coatings.

Type of coating	Surface roughness (R_a) (μm)	Adhesion strength (MPa)	Microhardness (HV0.05)
Protected coating	9.46 ± 2	27 ± 3	1000 ± 75
Unprotected coating	6.58 ± 1	11 ± 2	800 ± 55

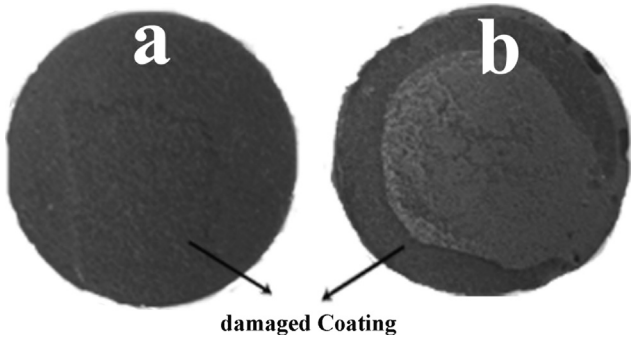

Fig. 5. The images of the samples after adhesion tests: (a) unprotected and (b) protected coating.

Fig. 4 shows the cross-section morphologies of the polished as-sprayed coatings obtained through the APS and ASPS processes. As shown in the figures, the surface roughness by the ASPS method is higher as compared to that of the APS method. Focus on the coating/substrate interface reveals that there is no delamination, holes, and separation for both coatings which demonstrates good adhesion of the coating to the substrate. As determined by image analysis, porosity content of the coatings formed using the APS process was $12 \pm 2\%$, while it was only $6 \pm 2\%$ for those obtained using the ASPS process.

Table 4 shows the results of roughness, microhardness, and adhesion strength measurements of coatings. As shown in Fig. 4, the roughness of spray coating using the ASPS method is higher than that of the unprotected coating. The relatively higher surface roughness (R_a) of the protected coating (9.46 μm), as compared to unprotected coating (6.58 μm), could be attributed to partially molten particles formed low-deformation impact on the surface as compared to fully molten particles [14,15]. The sprayed coating of the ASPS method contains a higher fraction of partially molten powder (Fig. 3), in comparison to the unprotected coating which is consistent with a relatively higher roughness of sprayed coating of the ASPS method.

The adhesion strength of the coatings sprayed by the ASPS and APS methods are about 27 and 11 MPa, respectively. However, the adhesion strength of ceramic coating produced by plasma spray on metallic substrates is about 15–20 MPa [14,16]. Therefore, the adhesion strength of the sprayed coating of the ASPS method is acceptable, implying that the chosen APS process parameters are suitable. The difference in adhesion strength is due to the cracks in the unprotected coating which tend to propagate along the weak zones with layer modes (splat boundaries) [17]. In addition, the structures of splat boundaries are interrupted by the area produced by the partially molten powder on the sprayed coating by the ASPS method. Crack propagation along the splat boundaries stopped as it reached to these zones and the coatings gained greater bond strengths [18]. Furthermore, the separated surfaces from adhesion test samples (Fig. 5) reveal that coating is not separated from the substrate and separation occurs from inside of the coating, indicating less adhesion among splats in comparison to the substrate. Besides, a comparison between the surface of the sprayed coating of the ASPS and APS methods revealed presence of fewer separated surfaces for the APS process, illustrating that the coating was separated from the surface layer – which might be a justification for the existence of surface cracks shown in Fig. 3.

According to Table 4, it can be understood that the coatings have considerable hardness. These values also demonstrate the existence of intermetallic compounds in the coating. Here, the Mo_5Si_3 phase should enhance the hardness of samples [19]; however, the hardness of the unprotected coating is less than that of the protected coating. The relative differences between

the hardness of coatings could be attributed to the presence of cracks, more defects, and less adhesion between splats in the APS process. This is consistent with studies of other researchers who reported that the defects and less cohesion between splats reduces the hardness [5,7].

4. Conclusions

(1) Applying the thermal spray process with ASPS equipment can significantly reduce the oxidation rate of the sensitive powders ($MoSi_2$).
(2) Thermal spray of $MoSi_2$ coating under argon shielding gas involves desired quality as compared to the unprotected coating.
(3) The hardness and adhesion strength of the protected coating are higher than those of the unprotected coating because of the less oxidation and consequently lower cracks and fewer defects.

References

[1] A. Vasudevan, J. Petrovic, A comparative overview of molybdenum disilicide composites, Materials Science and Engineering: A 155 (1) (1992) 1–17.
[2] R. Mitra, Mechanical behaviour and oxidation resistance of structural silicides, International Materials Reviews 51 (1) (2006) 13–64.
[3] Z. Yao, J. Stiglich, T. Sudarshan, Molybdenum silicide based materials and their properties, Journal of Materials Engineering and Performance 8 (3) (1999) 291–304.
[4] J.K. Yoon, J.M. Doh, J.Y. Byun, G.H. Kim, J.K. Lee, K.-T. Hong, Formation of $MoSi_2$–SiC composite coatings by chemical vapor deposition of Si on the surface of Mo_2C layer formed by carburizing of Mo substrate, Surface and Coatings Technology 173 (1) (2003) 39–46.
[5] G. Reisel, B. Wielage, S. Steinhäuser, I. Morgenthal, R. Scholl, High temperature oxidation behavior of HVOF-sprayed unreinforced and reinforced molybdenum disilicide powders, Surface and Coatings Technology 146 (2001) 19–26.
[6] R. Teghil, L. D'Alessio, A. Santagata, M. Zaccagnino, D. Ferro, Pulsed laser ablation of $MoSi_2$: gas phase analysis, Applied Surface Science 186 (1) (2002) 335–338.
[7] X. Fei, Y. Niu, H. Ji, L. Huang, X. Zheng, A comparative study of $MoSi_2$ coatings manufactured by atmospheric and vacuum plasma spray processes, Ceramics International 37 (3) (2011) 813–817.
[8] J.H. Yan, Y.M. Li, H.A. Zhang, S.W. Tang, Mechanical properties and high temperature oxidation behavior of La_2O_3–Mo_5Si_3/$MoSi_2$ composite, Chinese Journal of Nonferrous Metals 16 (10) (2006) 1730–1735.
[9] J.H. Yan, S.W. Tang, J.G. Xu, Microstructure and oxidation behavior of molybdenum disilicide coating prepared by air plasma sprayed, Materials Science Forum, Vol. 686, Trans Tech Publications, Switzerland, 583–588.
[10] M. Erfanmanesh, S.R. Bakhshi, Synthesis and characterization of nanocrystalline $MoSi_2$ by mechanical alloying and heat treating, Journal of Cluster Science 24 (1) (2013) 133–143.
[11] ASTM, Standard test method for adhesion or cohesion strength of thermal spray coatings, USA, 2001.
[12] K. Tee, L. Lu, M. Lai, In situ stir cast Al–TiB_2 composite: processing and mechanical properties, Materials Science and Technology 17 (2) (2001) 201–206.
[13] S. Bose, High temperature coatings, Elsevier Science and Technology Books, USA, 2007.
[14] H. Jamali, R. Mozafarinia, R. Shoja Razavi, R. Ahmadi-Pidani, M. Reza Loghman-Estarki, Fabrication and evaluation of plasma-sprayed nanostructured and conventional YSZ thermal barrier coatings, Current Nanoscience 8 (3) (2012) 402–409.
[15] A.N. Khan, J. Lu, Manipulation of air plasma spraying parameters for the production of ceramic coatings, Journal of Materials Processing Technology 209 (5) (2009) 2508–2514.
[16] L. Pawlowski, The science and engineering of thermal spray coatings, John Wiley & Sons, France, 2008.
[17] R. McPherson, A review of microstructure and properties of plasma sprayed ceramic coatings, Surface and Coatings Technology 39–40 (1) (1989) 173–181.
[18] M. Gell, E.H. Jordan, Y.H. Sohn, D. Goberman, L. Shaw, T.D. Xiao, Development and implementation of plasma sprayed nanostructured ceramic coatings, Surface and Coatings Technology 146–147 (2001) 48–54.
[19] B. Wielage, G. Reisel, A. Wank, G. Fritsche, Oxidation behaviour of molybdenum disilicide coating at 1500 °C, in: Proceedings of the International Thermal Spray Conference, Osaka, Japan, 2004, pp. 478–481.